

OPEN ACCESS

Medicinal Chemistry

Research Article

## Design, synthesis, molecular docking study, and biological evaluation of salicylaldimine derivatives as potential histone deacetylases inhibitors (HDACi) and anticancer agents

Heba M. Hesham, Deena S. Lasheen, Khaled A. Abouzid\*

Department of Pharmaceutical Chemistry, Faculty of Pharmacy, Ain Shams University, Cairo 11566, Egypt

### ABSTRACT

Despite the increased success rates of histone deacetylases inhibitors (HDACi) as potent anticancer agents, many metabolic obstacles face the hydroxamic acid-based HDAC inhibitors, which inspired us to develop non-hydroxamate HDAC inhibitors. Based on the established knowledge of the SAR of the reported HDAC inhibitors and based on the knowledge that salicylaldimine moiety is an established chelating agent, a series of salicylaldimine based HDAC inhibitors were designed, synthesized and biologically evaluated. The compound 14 in the present study showed considerable HDAC inhibition and potential antiproliferative activities on NCI cell lines rendering it as a good start for optimization that introduces a new class of non-hydroxamate HDAC inhibitors as potential anticancer agents.

**Keywords:** *Non-hydroxamate HDAC inhibitors; imines; salicylaldimine chelating agents*

\*Correspondence | Prof. Dr. Khaled A.M. Abouzid, Department of Microbiology and Immunology, Faculty of Pharmacy, Ain Shams University, African union organization street Abassia, Cairo 11566, Egypt. Email: [khaled.abouzid@pharma.asu.edu.eg](mailto:khaled.abouzid@pharma.asu.edu.eg)

Citation | Heba MH, Deena SL, Khaled AA. 2018. Design, synthesis, molecular docking study, and biological evaluation of salicylaldimine derivatives as potential HDAC inhibitors and anticancer agents. Arch Pharm Sci ASU 2(1): 1-15

DOI: [10.21608/APS.2018.18729](https://doi.org/10.21608/APS.2018.18729)

Online ISSN: 2356-8380. Print ISSN: 2356-8399.

Received 18 March 2018. Accepted 05 May 2018.

Copyright: ©2018 Hesham et al. This is an open-access article licensed under a Creative Commons Attribution 4.0 International License (CC BY 4.0), which permits unrestricted use, distribution, and reproduction in any medium, provided the original author(s) and source are credited

Published by: Ain Shams University, Faculty of Pharmacy

### 1. INTRODUCTION

Histone deacetylases inhibitors (HDACi) proved their potent cytotoxic effects and their capability in a reversal of resistance in many cancer cell lines by regulating the expression of a number of tumor suppressor genes that are involved in apoptosis of cancer cells [1]. DNA (deoxyribonucleic acid) is wrapped around the histones to be included inside the nucleus in the form of chromatin to form chromosomes as shown in Fig. 1. [2] HDACs catalyze the cleavage of the N-acetyl group from acetylated lysine residues located on the tails of the nucleosomal histones, so HDAC with the histone acetyltransferases (HAT) regulate the degree of acetylation and deacetylation of the histones

consequently the level of expression of the certain gene [3]. The overexpression of HDACs is directly linked to the poor prognosis of the cancer patient because they are responsible for removal of an acetyl group from the histones allowing interaction between negatively charged DNA and positively charged histone proteins, which lead to transcriptional silencing of tumor suppressor genes and apoptotic genes. Furthermore, many non-histone transcription factors such as heat shock protein-90 (HSP-90) and tubulin are the substrate for HDACs too [4]. As a result, HDACs control the level of expression of many oncogenes and apoptotic genes so control many cancer cellular processes such as cell proliferation, cell migration, cell death, and angiogenesis. In addition, many

studies have shown that HDAC inhibitors can restore the transcription of p53 protein that induces apoptosis for the resistant cancer cells [5]. In addition, HDAC inhibitors control the self-renewal of cancer stem cells by downregulation of Nanog expression which is one of the key transcription factors that has been shown to promote cancer progression by regulating cancer stem cells [6,7]. It was found that HDAC knockdown in cisplatin resistant cell lines (CisR) markedly downregulated Nanog and reversed the pluripotency of the cancer stem cells [7,8]. In addition, the HDAC inhibition with SAHA decreased survivin levels in CisR cell lines. Survivin is an important cell survival protein responsible for the inhibition of apoptosis in the cancer cells [7].

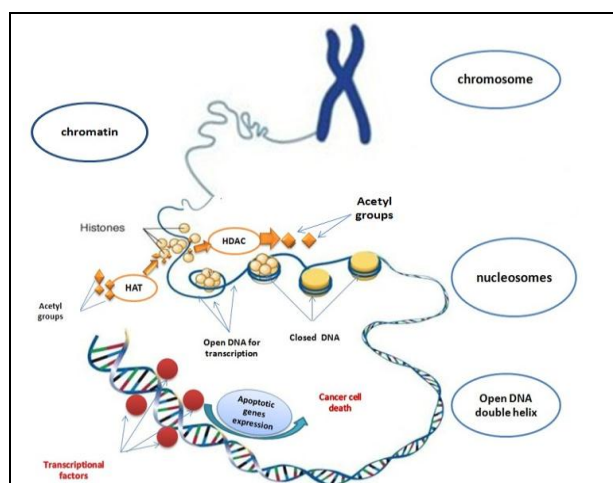


Fig. 1. mechanism of action of HDAC

HDACs comprise a family of 18 enzymes that is divided into four classes according to their sequence homology and domain organization. The class-I HDACs (HDAC1, 2, 3, and 8) located in the nucleus and expressed widely in various tissues and they are involved in gene expression. Class II HDACs are divided into two sub-groups, Class IIa (HDAC4, 5, 7, and 9) and Class IIb (HDAC6 and 10), and they are associated with cellular differentiation [9]. Class IIa HDACs shuttle between the cytoplasm and nucleus. Class IIb HDACs are situated in the cytoplasm and it is

found that HDAC-6 is involved in  $\alpha$ -tubulin deacetylation that may influence the mitotic process and other processes that depend on the acetylation pattern of the microtubular network [10]. In addition to all of the previous  $Zn^{2+}$  dependent HDACs, Class III HDACs are called sirtuins [SIRT1-SIRT7] and they are  $NAD^+$  dependent [11]. Class IV HDAC that comprises HDAC11, which is a unique member just because of the specific structure.

Up until now, the FDA showed in Fig. 2 has approved just four HDAC inhibitors. The 1<sup>st</sup> approved HDAC inhibitor was Suberoylanilide Hydroxamic acid SAHA (1) or Vorinostat under the trade name of Zolinza® that was developed by Merck for the treatment of refractory cutaneous T-cell lymphoma (CTCL). The 2<sup>nd</sup> one is Romidepsin (2) under trade name Istodax® in the market that was developed by Celgene pharmaceutical company for the treatment of CTCL and peripheral T-cell lymphoma (PTCL). In addition, in early 2015 the 3<sup>rd</sup> agent approved as HDAC inhibitor was panobinostat (3) and it was marketed under the name of Farydak® that was developed by Novartis to be used in oral combination with Bortezomib and Dexamethasone in patients with recurrent multiple myeloma. The 4<sup>th</sup> one is Belinostat (4) or called Beleodaq® in the market that was developed by Spectrum Pharmaceuticals to be used for the treatment of PTCL [12].

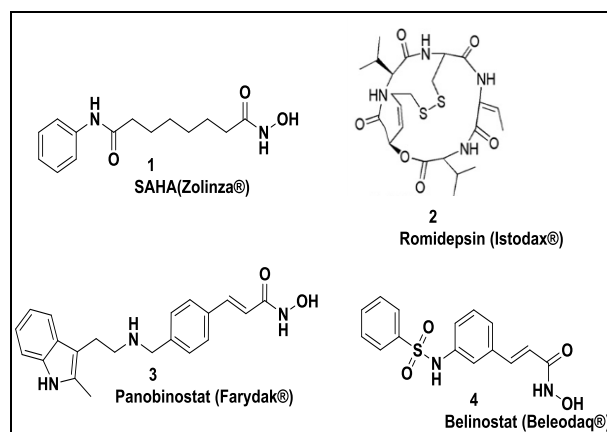
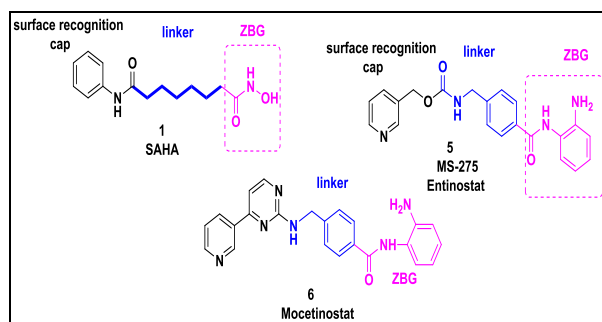


Fig. 2. FDA approved HDAC inhibitors

It is clear from **Fig. (3)** that HDAC inhibitors -except Romidepsin (**2**)- are sharing essential pharmacophoric structural features essential for activity [13]. The 1<sup>st</sup> feature is the hydrophobic capping group that interacts with the surface of the enzyme and aids in identification and binding of the compound with the enzyme. The 2<sup>nd</sup> feature is the linker that is essential for interaction with the enzymatic tunnel. The 3<sup>rd</sup> one is the zinc-binding group (ZBG) which is most commonly bidentate chelating group such as hydroxamic acid (HA) chelating group like in SAHA (**1**) which is potent HDAC inhibitor [14]. Despite this high potency of the hydroxamic acid as ZBG in HDAC inhibition, it suffers from *in vivo* instability as it is extensively metabolized in body rendering this potent HDAC inhibitor has two hours half-life then it is glucuronylated so it requires continuous injection [15]. That may lead to toxicity and off-target side effects including interaction with the cardiac potassium channel and mutagenic effects especially that HA-based HDAC inhibitors have pan HDAC inhibition so this increase the risk of cardiotoxicity. Therefore, there is increased interest in developing non-hydroxamate HDAC inhibitors that contain ZBG other than HA and capable of HDAC inhibition with more selectivity and fewer side effects [16].



**Fig. 3.** Pharmacophoric features of HDAC inhibitors [13]

There are many research groups working on the discovery of new non-hydroxamate HDAC inhibitors such as Entinostat (**5**) and Mocetinostat

(**6**) that bear 2-aminobenzamide as ZBG. Moreover, there are many reported ZBG for the design of non-hydroxamate HDAC inhibitors such as thiols as in compound (**7**), electrophilic ketone as in compound (**8**), Mercaptoamides (**9**), Sulfones (**10**) and Phosphones (**11**) shown in **Fig. (4)**.

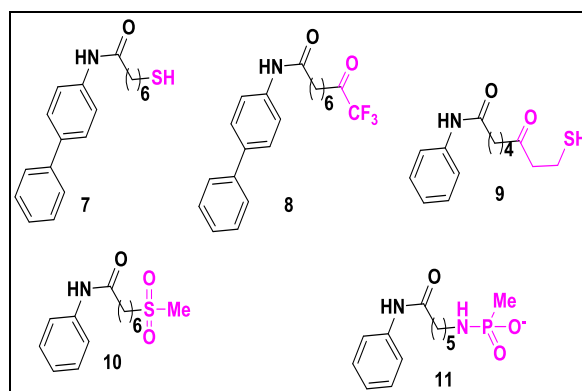


**Fig. 4.** Some examples of non-hydroxamate HDAC inhibitors [16]

In our study, we have explored the reported chelating agent salicylaldimine [17] and other imine analogs 2-thiophene imine and 2-pyridine imine to be the ZBGs [18,19] which connected via phenyl linker to different surface recognition caps containing urea, sulfonamides, piperazine and benzthiazole to form novel non-hydroxamate HDAC inhibitors targeting the cancer cells. In addition, we report the synthesis, the assay of percent inhibition of HDAC-6 isoenzyme at 10  $\mu$ M and cancer cell percent growth inhibition on the NCI cell lines panel at a single dose (**Table 2 & Fig. 11**).

## 2. Design and molecular docking study

Upon the basis of the well-established knowledge of the structural parameters (cap, linker, ZBG) that are essential for HDACs inhibitory activity, we chose to investigate the design of some new salicylaldimine-based HDACi that might retain the desired zinc chelating activity instead of the hydroxamic acid chelating group. Salicylaldimine is reported as a popular bidentate ligand that chelates with the

different metal like iron and zinc. In addition, we investigated the other imines as analogs for salicylaldimine by replacing the ortho hydroxyl group with either cyclic nitrogen or cyclic sulfur to test the ability of thiophene-2-ylmethanimine as in compound **17** and compound **28** and we also tried the pyridine-2-ylmethanimine as in compound **16** and compound **27** to act as novel zinc chelating groups. Furthermore, we chose versatile linkers for the designed compounds such as sulfonamides, urea or piperazine that connect the ZBG to different surface recognition cap such as phenyl as in compounds **25**, **27**, **28**, and 4-isopropylphenyl as in compound **14**, diphenyl in compounds **26** and compounds **24**, **28**, benzthiazole cap in compound **21**, naphthyl in compounds **15**, **16**, and **17**.

These designed compounds were further evaluated by molecular docking via the semi-empirical forcefield based Autodock Vina software in HDAC-6 isoenzyme that is co-crystallized with Trichostatin (TSA) (PDB code: 5edu). The pose generation process was validated by calculation the root mean square standard deviation (RMSD) between the cocrystallized TSA and the docked one. The resultant RMSD was 1.293, which reflects the ability of this docking engine to dock the compounds inside the active site of HDAC-6 with the right pose as shown in **Fig. 5**.

The co-crystallized TSA showed essential interactions with the amino acids His611, Phe620, and tyr782 inside HDAC-6 binding site as shown in **Fig. 6**. Most of our designed compounds showed very similar binding mode as TSA with comparable docking score to it especially the salicylaldimine derivatives.

The designed compound **14** showed binding Vina score of 28, which is comparable to the lead TSA binding, score 31. Moreover, it retained the essential binding features of TSA binding such as

zinc binding, hydrogen bonding with HIS<sub>611</sub>, and pi-pi interactions with Phe<sub>620</sub> and with PHE<sub>680</sub> in addition as shown in **Fig. 7**. The second promising salicylaldimine derivative with docking score of 27.56 was compound **27** (**Fig. 8**) that showed very similar binding modes to the lead TSA with zinc and PHE<sub>620</sub> and formed extra interactions with ASP<sub>649</sub> and HIS<sub>610</sub>. Furthermore, the compound **24** (**Fig. 9**) showed docking scores of 27.2 with retaining the essential key interactions and with the formation of an extra hydrogen bond with TYR<sub>782</sub>.

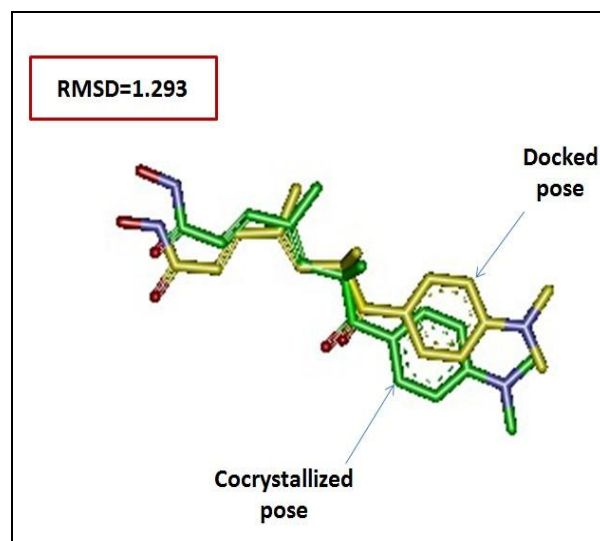


**Fig. 5.** Evaluation of the pose prediction accuracy of the docking software autodock vina

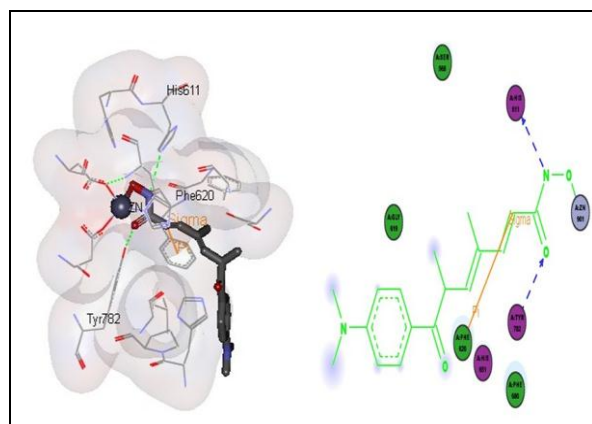


**Fig. 6.** 2D and 3D Binding pattern of the co-crystallized Trichostatin

The use of hydrophobic moieties as capping group such as naphthyl in compounds **15**, **16**, **17** and 6-methoxy benzothiazole as in compound **21** (**Fig. 10**) rendered the caps more surface binder with extra interaction with HIS<sub>651</sub>. These findings from molecular docking by autodock vina directed us to proceed in the chemical synthesis of the designed compounds and their further biological evaluation.

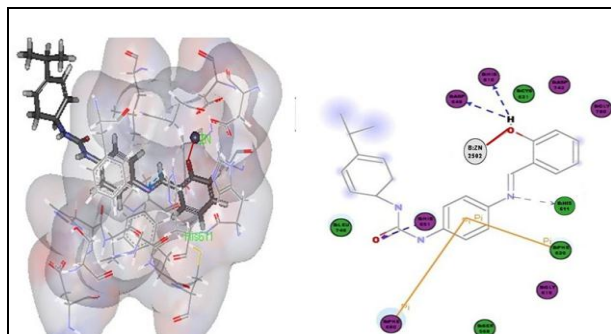


**Fig. 7.** 2D and 3D Binding pattern of the designed compound 14

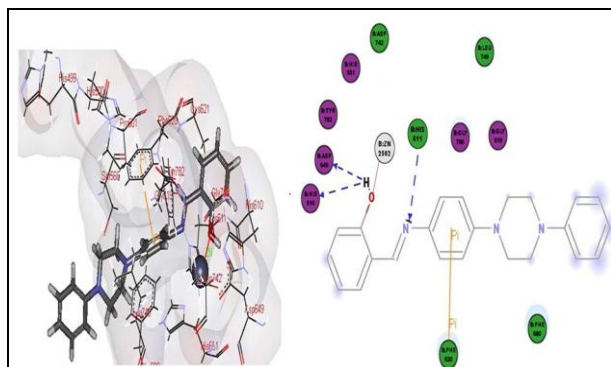


**Fig. 8.** 2D and 3D Binding pattern of the designed compound 27

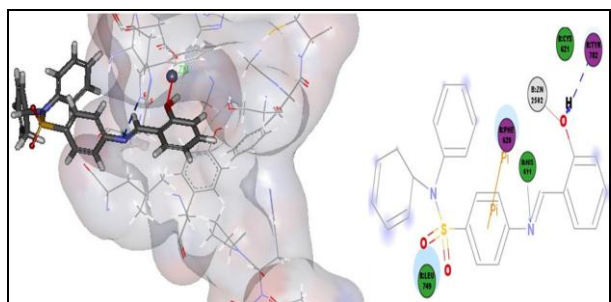


**Fig. 9.** 2D and 3D Binding pattern of the designed compound 24

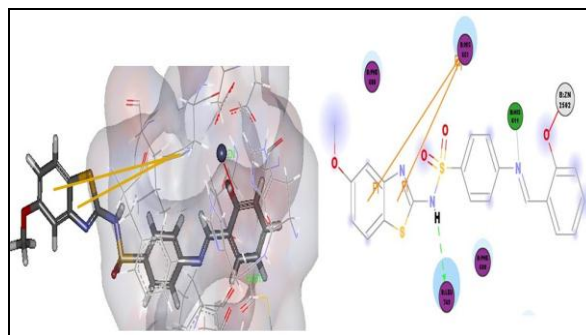
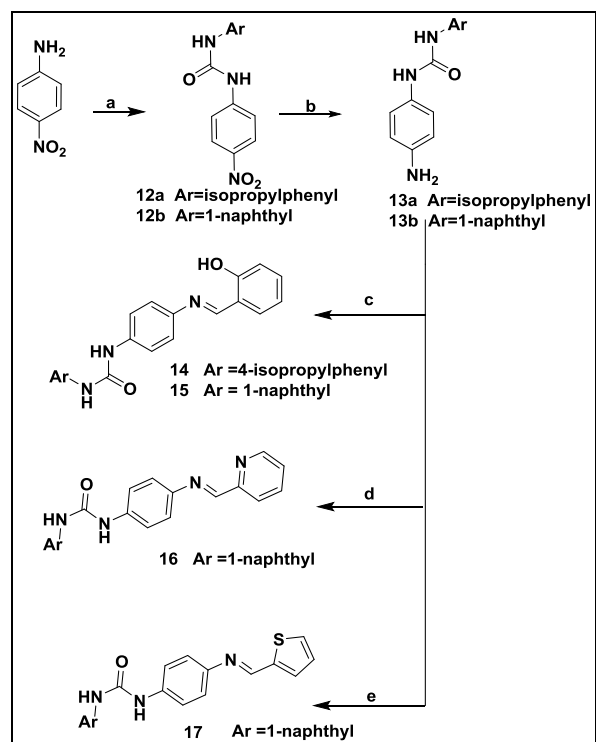


**Fig. 10.** 2D and 3D Binding pattern of the designed compound 21

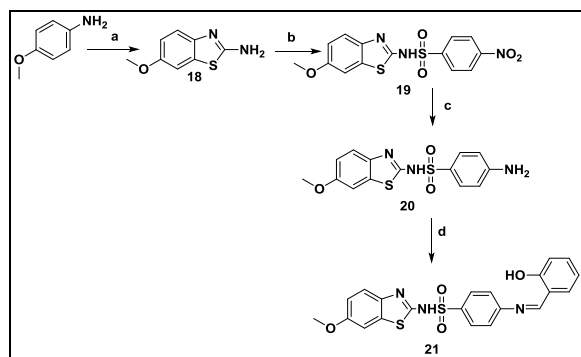
### 3. Chemistry

After the promising findings of the molecular docking study for our designed compound, four schemes were designed for synthesis of these compounds. **The first scheme** was for the synthesis of biaryl urea-based caps and imine based ZBGs. The synthesis of biaryl ureas was done by reacting the 4-nitroaniline with either 1-naphthyl isocyanate or 4-isopropylphenyl isocyanate [20]. The resultant nitro containing ureas were reduced to the corresponding amines via catalytic hydrogenation using 10% Pd loaded on charcoal [21] then the resulting amines were condensed either with salicylaldehyde, thiophene-2-carboxaldehyde or pyridine-2-carboxaldehyde under Dean-stark apparatus in toluene to afford the corresponding imines [22].

**The second scheme** was for the synthesis of 6-methoxy benzothiazole based cap from 4-methoxyaniline using potassium thiocyanate and bromine to make oxidative ring closure in acetic acid [23], and then the resultant amine intermediate was reacted with nitrobenzenesulfonylchloride in pyridine to afford the corresponding sulfonamide derivatives [24]. The resultant intermediate compound **19** then reduced via catalytic hydrogenation affording the corresponding amine that reacted then with salicylaldehyde affording compound **21**.



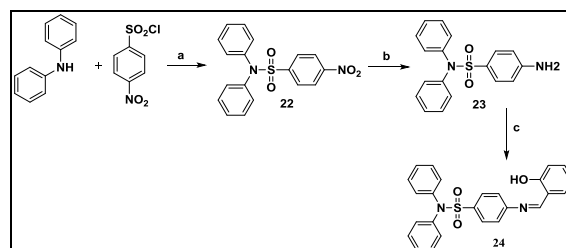
**Scheme 1.** Reagents and conditions (a) reflux with Aryl isocyanates in THF at 60 °C overnight (b) reflux with Fe/ammonium chloride in ethanol/water for 4 h (c) reflux with salicylaldehyde in ethanol/glacial acetic acid for 24 h (d) reflux with pyridine-2-carboxaldehyde in ethanol/glacial acetic acid for 24 h (e) reflux with thiophene-2-carboxaldehyde in ethanol/ glacial acetic acid for 24 h.



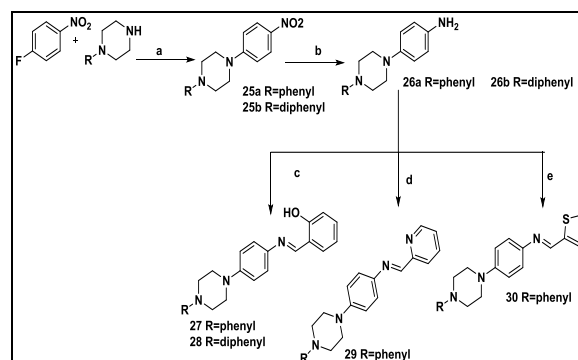
**Scheme 2:** Reagents and conditions (a) stirring with KSCN, Br<sub>2</sub>, glacial acetic acid in ice bath (b) stirring with p-nitrobenzene sulfonyl chloride in pyridine for 2 days at room temperature (c) reflux with SnCl<sub>2</sub> in ethanol for 6 h (d) reflux with salicylaldehyde in ethanol/glacial acetic acid mixture for 12 h.

**The third scheme** was designed to synthesize compound **24** that contains diphenyl

cap and sulfonamide linker and salicylaldimine ZBG. This scheme begins with the diphenylamine that was reacted with the nitrobenzene sulfonyl chloride in pyridine to afford the intermediate compound **22**, which then reduced to afford the corresponding amine that then reacted with the salicylaldehyde to produce the imine derivative.



**Scheme 3.** Reagents and conditions (a) stirring in pyridine for 2 days (b) reflux with SnCl<sub>2</sub> in ethanol for 6 h (c) reflux with salicylaldehyde in ethanol/glacial acetic acid for 6 h.



**Scheme 4.** Reagents and conditions (a) reflux with K<sub>2</sub>CO<sub>3</sub> in DMF (b) H<sub>2</sub>/Pd/C (c) reflux with salicylaldehyde in ethanol-acetic acid mixture till precipitation (d) reflux with pyridine 2-carboxaldehyde in a mixture of ethanol-acetic acid till precipitation (e) reflux with thiophene 2-carboxaldehyde in a mixture of ethanol-acetic acid till precipitation.

**The fourth scheme** was designed to synthesize the piperazine derivatives that have either salicylaldimine as ZBG, thiophene-2-ylmethanimine or pyridine-2-ylmethanimine. This scheme begins with the nucleophilic aromatic substitution of the phenylpiperazine on 4-fluoronitrobenzene in basic condition and in DMF as solvent [25]. Then the resultant nitro derivative was

reduced via catalytic hydrogenation to afford the aniline derivative that was reacted with salicylaldehyde to give compound **27** and with thiophene-2-carboxaldehyde to afford compound **29** and with pyridine-2-carboxaldehyde to yield compound **30**

#### 4. Biological evaluation

##### 4.1. *In vitro* HDAC inhibition assay

The synthesized compounds were tested for their inhibitory activity towards HDAC-6 isoform in Bioscience Company (**Table 1**), and they were selected by NCI for determination of their antiproliferative activities against the NCI panel of 60 tumor cell lines. On the HDAC-6 isoenzyme, compound **14** showed the most potent HDAC-6 inhibition with percent inhibition of 63% at 10  $\mu$ M concentration. Replacing the isopropyl phenyl cap with naphthyl cap in compound **15** diminished the percent inhibition to be 5%, which suggest that 1-naphthyl moiety may interfere with the entrance of HDAC tunnel. Furthermore, replacing the salicylaldimine chelating group with thiophene-2-ylmethanimine in compound **16** or pyridine-2-ylmethanimine in compound **17** rendered the HDAC percent inhibition to be 0% for both compounds. In addition, 5-methoxy benzothiazole capping group may interfere with the entrance of HDAC tunnel too as the HDAC percent inhibition resulted was 12% in the compound **21**. Compound **24** that contains biphenyl sulfonamide cap showed considerable HDAC percent inhibition of 52%. Interestingly, compound **27** that contains piperazine as linker showed 58% HDAC inhibition but replacing the salicylaldimine-chelating group with pyridine-2-ylmethanimine in compound **29** and thiophene-2-ylmethanimine in compound **30** caused a severe decline in HDAC inhibitory activity to be 3% and 0%, respectively. Replacing the phenylpiperazine with phenylpiperazine moiety in compound **28**

decreased the percent inhibition to be 29% instead of being 58 % in compound **27**.

**Table 1.** Inhibitory activities of the Compounds on HDAC-6 Activity

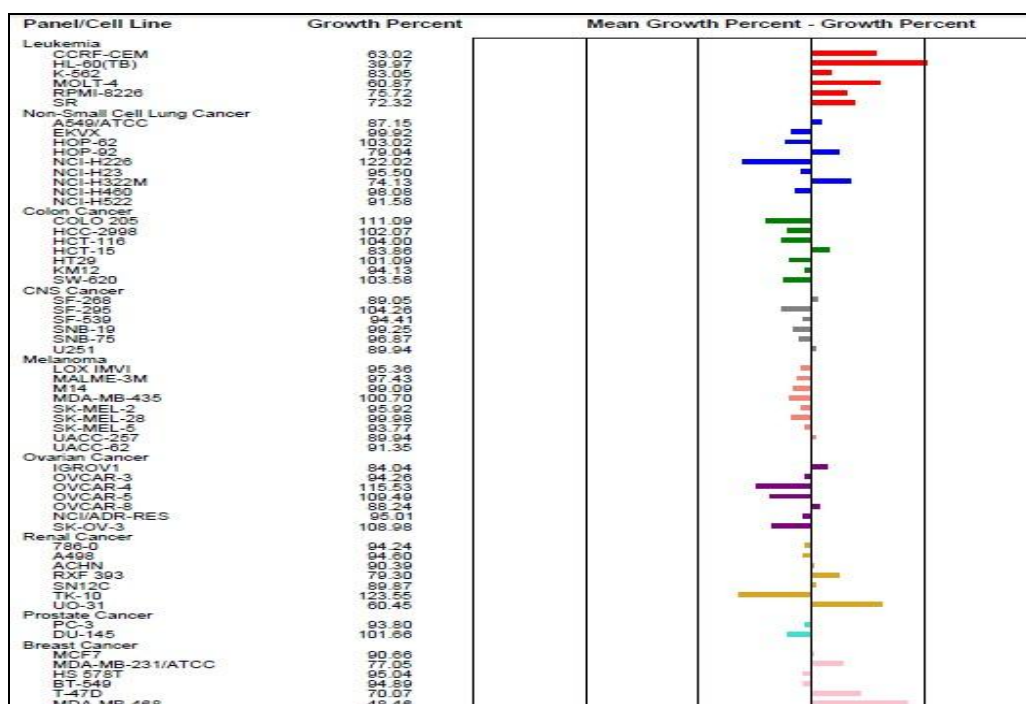
Compound ID #	Percentage Inhibition (%)
HDAC-6	
<b>14</b>	63
<b>15</b>	5
<b>16</b>	0
<b>17</b>	0
<b>21</b>	12
<b>24</b>	52
<b>27</b>	58
<b>28</b>	29
<b>29</b>	3
<b>30</b>	0
<b>SAHA</b>	100

##### 4.2. Antiproliferative activity

The designed compounds were selected by NCI to be tested on the 60-cell panel and the results were represented in either tabular form or one dose graph. The compound that showed most potent antiproliferative activity at 10  $\mu$ m single dose was compound **14** that induced 60% inhibition for HL-60 cell line of leukemia that overexpresses the HDACs. Moreover, compound **14** showed 40% inhibition to CCR-CEM and Molt-4 cell lines of leukemia and UO-31 cell line of renal cancer rendering it promising start for further optimization of the antiproliferative activity and HDAC inhibitory activity. Interestingly, compound **24** showed 70% inhibition on UACC-62 cell line of melanoma. Furthermore, compound **27** showed 49% inhibition on HI-60 cell line of leukemia that overexpresses HDACs and 47% inhibition on BT-549 cell line of breast cancer rendering it interesting for further antiproliferative optimization.

**Table 2.** The percent growth inhibition on some of NCI cell lines

Compound	CCRF-CEM	HL-60 (TB)	MOLT-4	NCI-H522	UO-31	UACC-62	SK-OV-3	BT-549	MDA-MB-468
	%inhibition								
14	37	60	40	9	40	9	-	6	52
15	20	20	10	8	19	8	-	15	13
16	17	12	9	10	15	10	-	2	-
17	12	25	9	15	18	12	-	12	-
21	3	3	9	35	5	-	25	5	-
24	-	7	9	10	15	70	3	6	9
27	38	49	7	5	14	5	36	47	-
28	24	21	13	13	13	1	13	23	-
29	13	12	10	20	18	2	31	25	-
30	34	21	18	20	15	7	30	30	8

**Fig. 11.** One dose graph that represents the effect of compound 14 on the percent growth of the NCI cell lines

## 5. Conclusion

In conclusion, we have designed and synthesized a new class of non-hydroxamate HDAC inhibitors exploring salicylaldehyde moiety and other imines as new zinc chelating

group. The idea was explored first via molecular docking inside HDAC-6 before the synthesis and the *in vitro* assay. The good correlation between the docking results and biological assays results rendered the use of autodock vina as a useful tool in the design of further HDAC-6 analogs.

Moreover, the synthesized compounds were selected to be tested for their antiproliferative activities against the NCI panel of 60 tumor cell lines. Compound **14** that possesses isopropylphenyl moiety as capping group and urea as linker and salicylaldimine as ZBG exhibited considerable HDAC-6 percent inhibition and potential to be effective anticancer after further optimization. In addition, compound **24** and compound **27** that have salicylaldimine moiety as a chelating group also exhibited considerable HDAC inhibition and antiproliferative activities that strongly supports the idea of using the salicylaldimine as ZBG. We suggest a modification of either the linker length to be longer than used in compound **14** or inverting the imine to make the nitrogen besides the hydroxyl with no carbon spacer that may improve the chelation power resulting in more potent HDAC inhibition and anticancer activity.

## 6. Experimental

### 6.1. Materials and instrumentation

Starting materials and reagents were purchased from Sigma-Aldrich or Alfa-Aesar Organics and used without further purification. Solvents were purchased from Fisher Scientific or Sigma-Aldrich and used without further purification. Reactions were monitored by analytical TLC, performed on silica gel 60 F254 packed on aluminum sheets, purchased from Merck, with visualization under UV light (254 nm). Flash column chromatography was performed using silica gel (230-400 mesh) purchased from Sigma-Aldrich. Melting points were recorded on Stuart Scientific apparatus and were uncorrected. HNMR spectra were recorded in  $\delta$  scale given in ppm on a Bruker 400 MHz spectrophotometer and referred to TMS at Center for Drug Discovery Research and Development, Ain Shams University. The hydrogenation process

was carried out using hydrogenator (Parr Shaker) apparatus at Ain Shams University.

### 6.2. General procedure for the synthesis of biaryl urea derivatives (12a-13b) (method A)

To a solution of *p*-nitroaniline (1 g, 7.5 mmol; 1 equiv.) in dry dioxane (10 mL), the appropriate isocyanate (8.6 mmol; 1.2 equiv.) was added and the mixture was stirred at room temperature overnight. The formed solid was collected by filtration, washed with dioxane, allowed to dry.

### 6.3. General procedure of reduction via catalytic hydrogenation (method B) (13a, 13b, 20, 23, 26a, 26b)

To a solution of the appropriate nitrophenyl urea derivative (7 mmol) in methanol (100 mL), Pd-C (0.1 g, 10%) was added and the mixture was stirred under H<sub>2</sub> at room temperature at 45 Bar for 2 h. After removing the catalyst by filtration over celite, the filtrate was concentrated under vacuum and dried to afford the crystals.

### 6.4. General procedure for imine synthesis (method C) (14, 15, 16, 17, 21, 24, 27, 28, 29, 30)

To a solution of the appropriate amine (1.32 mmol) in dried toluene (10 mL) in presence of 1 mL glacial acetic acid, 0.2 mL (1.32 mmol) of the appropriate aldehyde. The mixture is refluxed under dean stark apparatus until precipitate is formed. The formed solid was collected by filtration and washed with toluene.

### 6.5. General Method for the synthesis of sulfonamides (Method D) (19, 22)

To a solution of the appropriate amine (3.5 mmol) in pyridine (5 mL) placed in an ice bath, 1.2 equivalent of 4-nitrobenzene sulfonyl chloride (4 mmol) was added portion wise and left stirring for 48 h at room temperature. After that, the solution is poured on ice/HCl and the

formed solid was collected by filtration and washed with diethyl ether.

#### 6.5.1. 1-(4-Isopropylphenyl)-3-(4-nitrophenyl) urea (12a)

To a solution of *p*-nitroaniline (1 g, 7.5 mmol: 1 equiv.) in dry dioxane (10 mL), 1.57 mL of 4-isopropylphenyl isocyanate (8.6 mmol; 1.2 equiv.) was added as in method A to give yellow solid, yield 83%, m.p 105-106 °C.

#### 6.5.2. 1-(Naphthalene-1-yl)-3-(4-nitrophenyl) urea (12b)

To a solution of *p*-nitroaniline (1 g, 7.5 mmol: 1 equiv.) in dry dioxane (10 mL), 1.7 ml of 1-naphthyl isocyanate (8.6 mmol; 1.2 equiv.) was added as in method A to give brilliant yellow solid, yield 75%, m.p 96-98 °C.

#### 6.5.3.1-(4-Aminophenyl)-3-(4-isopropylphenyl) urea (13a)

Catalytic hydrogenation was performed on a solution of **12a** (7 mmol) in methanol (10 mL) as in method B to afford white crystals with yield 90% and with m.p of 91-92 °C.

#### 6.5.4. 1-(4-Aminophenyl)-3-(naphthalene-1-yl) urea (13b)

Catalytic hydrogenation was performed on a solution of **12b** (3.5 mmol) in methanol (10 mL) as in method B to afford white crystals with yield 92% and with m.p of 145-148 °C.

#### 6.5.5. 1-(4-((2-Hydroxybenzylidene) amino) phenyl)-3-(4-isopropylphenyl) urea (14)

To a solution of **13a** (1.11 mmol) 0.13 mL of salicylaldehyde(1.11 mmol) was added as in method C then purified via flash column using the system (hexane: ethyl acetate 8:2) to afford yellow powder with yield of 55% and m.p of 122 °C; <sup>1</sup>H NMR (400 MHz, DMSO-d<sub>6</sub>) δ 13.34

(s, 1H), 9.00 (s, 2H), 8.96 (s, 1H), 8.80 (s, 1H), 7.63 (d, *J* = 7.6 Hz, 1H), 7.56 (d, *J* = 8.3 Hz, 2H), 7.39 (dd, *J* = 12.2, 8.0 Hz, 5H), 7.16 (d, *J* = 8.0 Hz, 2H), 6.97 (dd, *J* = 11.9, 7.5 Hz, 2H), 2.84 (hept, *J* = 7.0 Hz, 1H), 1.19 (d, *J* = 7.0 Hz, 6H).

#### 6.5.6.1-(4-((2-Hydroxybenzylidene)amino)phenyl)-3-(naphthalen-1-yl)urea (15)

To a solution of **13b** (1.11 mmol) , 0.13 mL of salicylaldehyde(1.11 mmol) was added as in method C and purified via flash column using the system (hexane:ethyl acetate 8:2)to afford orange solid with yield of 35% and m.p of 112-115 °C; <sup>1</sup>H NMR (400 MHz, DMSO-d<sub>6</sub>) δ 13.34 (s, 1H), 9.23 (s, 2H), 8.99 (s, 1H), 8.83 (s, 1H), 8.72 – 8.46 (m, 1H), 8.22 – 7.80 (m, 2H), 7.75 – 7.33 (m, 9H), 7.23 (s, 1H), 6.99 (d, *J* = 12.5 Hz, 1H), 6.56 (d, *J* = 24.0 Hz, 1H).

#### 6.5.7.1-(Naphthalen-1-yl)-3-(4-((pyridin-2-ylmethylene) amino) phenyl) urea (16)

To a solution of **13b** (1.11 mmol) 0.11 mL of pyridine-2-carboxaldehyde (1.11 mmol) was added as in method C then purified via flash column using the system (hexane:ethyl acetate 8:2) to produce buff powder with yield of 40% and m.p of 112-115 °C ; <sup>1</sup>H NMR (400 MHz, DMSO-d<sub>6</sub>) δ 9.21 (s, 1H), 8.96 (s, 1H), 8.80 (s, 2H), 8.73 (d, 1H), 8.30 – 7.89 (m, 5H), 7.71 – 7.39 (m, 9H).

#### 6.5.8.1-(Naphthalen-1-yl)-3-(4-((thiophen-2-ylmethylene) amino) phenyl) urea (17)

To a solution of **13b** (1.11 mmol) 0.12 mL of thiophene-2-carboxaldehyde (1.11mmol) was added as in method C to afford white powder after flash column using the system (hexane: ethyl acetate 8:2) with yield of 29% and m.p of 112 °C; <sup>1</sup>H NMR (400 MHz, DMSO-d<sub>6</sub>) δ 9.16 (s, 1H), 8.97 (s, 1H), 8.82 (s, 1H), 8.61 (s, 1H), 8.23 – 7.88 (m, 3H), 7.67 (d, *J* = 9.4 Hz, 1H),

7.53 (d,  $J = 37.2$  Hz, 6H), 7.27 (d,  $J = 32.4$  Hz, 2H), 6.58 (d,  $J = 13.8$  Hz, 1H).

#### 6.5.9. 6-Methoxybenzo[*d*]thiazol-2-amine (18)

To a stirred solution of 4-methoxy aniline (8 mmol) and 3.75 g potassium thiocyanate (7 equivalents) in glacial acetic acid (10 mL) placed in ice bath bromine solution (80 mmol) was added portion wise then left stirring overnight. Then the solution is poured and the formed solid is collected by filtration and washed by DEE to afford gray solid with yield 62% and m.p of 161-163 °C.

#### 6.5.10. N-(6-methoxybenzo[*d*]thiazol-2-yl)-4-nitrobenzenesulfonamide (19)

To a solution of **18** (3.5 mmol) in pyridine (5 mL) placed in an ice bath, 1.2 equivalents of 4-nitrobenzene sulfonyl chloride (4 mmol) as in method D to afford orange solid with a yield of 70% and m.p of 154-155 °C.

#### 6.5.11. 4-Amino-N-(6-methoxybenzo[*d*]thiazol-2-yl) benzenesulfonamide (20)

To a solution of the nitro compound **19** (7 mmol) in methanol (100 mL), Pd-C (0.1 g, 10%) as in method B to afford white crystals with a yield of 52% and m.p of 130-133 °C.

#### 6.5.12. 4-((2-Hydroxybenzylidene) amino)-N-(6-methoxybenzo[*d*]thiazol-2-yl) benzenesulfonamide (21)

To a solution of **20** (1.11 mmol) 0.12 mL of salicylaldehyde (1.11 mmol) was added and continued as in method C then purified via flash column using the system (hexane: ethyl acetate 8:2) to afford yellow powder with yield of 48% and m.p of 157 °C;  $^1\text{H NMR}$  (400 MHz, DMSO-*d*6)  $\delta$  13.20 (s, 1H), 8.41 (s, 1H), 8.30 – 7.78 (m, 5H), 7.48 (s, 2H), 7.26 (d,  $J = 15.5$  Hz, 2H), 7.00 (s, 2H), 3.97 – 3.67 (s, 5H).

#### 6.5.13. 4-Nitro-N, N-diphenylbenzene sulfonamide (22)

To a solution of the diphenylamine (3.5 mmol) in pyridine (5 mL) placed in an ice bath, 1.2 equivalent of 4-nitrobenzene sulfonyl chloride (4 mmol) was added and continued as in method D to afford buff solid with a yield of 88% and m.p of 165-168 °C.

#### 6.5.14. 4-amino-N, N diphenyl benzene sulfonamide (23)

To a solution of the **22** (7 mmol) in methanol (100 mL), Pd-C (0.1 g, 10%) was added and continued as mentioned in method B to afford white crystals yield 85% and m.p 134 °C.

#### 6.5.15. 4-((2-Hydroxybenzylidene) amino)-N, N-diphenyl benzenesulfonamide (24)

To a solution of the **23** (1.32 mmol) in methoxyethanol (10 mL), 0.18 mL (1.32 mmol) of the salicylaldehyde was added and continued as in method C then purified via flash column using the system (hexane: ethyl acetate 8:2). That was to afford buff solid with yield of 55% and m.p of 103 °C;  $^1\text{H NMR}$  (400 MHz, DMSO-*d*6)  $\delta$  12.47 (s, 1H), 9.02 (s, 2H), 7.73 (d,  $J = 8.3$  Hz, 3H), 7.58 (d,  $J = 8.2$  Hz, 2H), 7.46 – 7.39 (m, 6H), 7.34 (s, 6H), 7.01 (d,  $J = 7.6$  Hz, 2H).

#### 6.5.16. 1-(4-Nitrophenyl)-4-phenylpiperazine (25a)

To a mixture of phenylpiperazine (3.5 mmol) and fluronitrobenzene (3.5 mmol) in DMF (5 mL), 0.65 g of dried potassium carbonate (3 equivalents) was added and the mixture was refluxed for 12 h then the solution was poured onto ice to afford orange solid which was collected by filtration and washed with diethyl ether with yield of 88% and m.p of 108 °C.

#### 6.5.17. 4-(4-Phenylpiperazine-1-yl) aniline (26a)

To a solution of 25a (7 mmol) in methanol (100 mL), Pd-C (0.1 g, 10%) was added and continued as in method B to afford grayish solid with a yield of 88% and m.p of 137 °C.

#### 6.5.18. 2-(((4-(4-Phenylpiperazine-1-yl) phenyl) imino) methyl) phenol (27)

To a solution of the 26a (1.32 mmol), 0.15 mL (1.32 mmol) of salicylaldehyde was added as in method C then purified via flash column using the system (hexane: ethyl acetate 8:2). That was to afford golden yellow solid with yield of 70% and m.p of 102 °C; <sup>1</sup>H NMR (400 MHz, DMSO-d<sub>6</sub>) δ 13.49 (s, 1H), 8.96 (s, 2H), 7.60 (dd, *J* = 7.7, 1.7 Hz, 1H), 7.39 (dd, *J* = 8.9, 7.3 Hz, 3H), 7.26 (dd, *J* = 8.5, 7.1 Hz, 2H), 7.15 – 7.04 (m, 2H), 7.02 (d, *J* = 8.1 Hz, 2H), 7.00 – 6.89 (m, 2H), 6.82 (t, *J* = 7.3 Hz, 1H), 3.30 (d, *J* = 6.8 Hz, 8H)

#### 6.5.19. N-(4-(4-Phenylpiperazin-1-yl) phenyl)-1-(pyridin-2-yl) methanimine (29)

To a solution of the 26a (1.32 mmol), 0.15 mL (1.32 mmol) of pyridine-2-carboxaldehyde was added as in method C then purified via flash column using the system (hexane: ethyl acetate 8:2) to afford white solid with yield of 48% and m.p of 111 °C; <sup>1</sup>H NMR (400 MHz, Chloroform-d) δ 8.72 (d, *J* = 4.9 Hz, 1H), 8.69 (s, 2H), 8.22 (d, *J* = 7.8 Hz, 1H), 7.82 (t, *J* = 7.7 Hz, 1H), 7.42 – 7.27 (m, 5H), 7.04 (t, *J* = 8.6 Hz, 4H), 6.93 (t, *J* = 7.3 Hz, 1H), 3.52 – 3.33 (m, 8H).

#### 6.5.20. N-(4-(4-phenylpiperazin-1-yl) phenyl)-1-(thiophen-2-yl) methanimine (30)

To a solution of the 26a (1.32 mmol), 0.12 mL (1.32 mmol) of thiophene-2-carboxaldehyde was added as in method C then purified via flash column using the system (hexane: ethyl acetate 8:2) to afford off-white solid with yield of 36%

and m.p of 123 °C; <sup>1</sup>H NMR (400 MHz, Chloroform-d) δ 8.63 (s, 2H), 7.48 (dd, *J* = 9.0, 4.4 Hz, 2H), 7.39 – 7.22 (m, 4H), 7.15 (t, *J* = 4.3 Hz, 1H), 7.03 (d, *J* = 8.2 Hz, 4H), 6.93 (t, *J* = 7.4 Hz, 1H), 3.40 (s, 8H).

#### 6.5.21. 1-Benzhydryl-4-(4-nitrophenyl) piperazine (25b)

To a mixture of 1-benzhydrylpiperazine (3.5 mmol) and fluronitrobenzene (3.5 mmol) in DMF (5 mL), 0.65 g of dried potassium carbonate (3 equivalents) was added and continued as in compound 25a to afford yellow solid with a yield of 92% and m.p of 112 °C.

#### 6.5.22. 4-(4-Benzhydryl piperazine-1-yl) aniline (26b)

To a solution of 25b (7 mmol) in methanol (100 mL), Pd-C (0.1 g, 10%) was added and continued as in method B to afford off-white solid with a yield of 80% and m.p of 145 °C.

#### 6.5.23. (E)-2-(((4-(4-benzhydrylpiperazin-1-yl)phenyl) imino)methyl) phenol (28)

To a solution of the 26b (1.32 mmol), 0.15 mL (1.32 mmol) of salicylaldehyde was added as in method C, then purified via flash column using the system (hexane:ethyl acetate 8:2) to afford yellow solid with yield of 50% and m.p of 110 °C; <sup>1</sup>H NMR (400 MHz, Chloroform-d) δ 13.60 (s, 1H), 8.64 (s, 2H), 7.48 (s, 4H), 7.30 (s, 10H), 6.99 (d, *J* = 32.5 Hz, 4H), 4.30 (s, 1H), 3.26 (s, 4H), 2.60 (s, 4H).

### 6.6. Molecular modelling

Molecular docking study was performed using autodock vina docking software interface and while protein and ligands preparation prior docking process was conducted through Accelrys discovery studio 2.5 via prepare protein and prepare ligands protocols.

### 6.6.1. Preparation of protein

The X-ray crystal structure of HDAC-6 co-crystallized with Trichostatin (TSA) was obtained from the Protein Data Bank at the Research Collaboration for Structural Bioinformatics (RCSB) website [www.rcsb.org] (PDB code: 5 edu) and loaded in Accelrys discovery studio 2.5. The protein structure was prepared using the default protein preparation tools integrated into the software. This was accomplished by adding hydrogen atoms to the amino acid residues, completing the missing residues, and applying force field parameters by using CHARMM forcefield 256. All of the protein structure was minimized using 500 steps employing SMART minimizer algorithm. The heavy atoms other than hydrogen were kept fixed during the minimization process. The whole enzyme was defined as the receptor. In addition, binding pocket together with the surrounding amino acid residues was identified. The ligand structure was removed from the binding sites.

### 6.6.2. Ligand preparation for docking

Ligands structures were constructed using the default sketching tools of Accelrys discovery studio 2.5 and then the ligands were prepared using Ligand preparation protocol of Accelrys Discovery Studio. The ionization pH was adjusted to 7.4, hydrogen atoms were added and no isomers or tautomers were generated from the ligands

### 6.6.3. Docking process

The autodock vina protocol performs random searching for poses via a genetic algorithm to find poses close to the bioactive form. Then the scoring step is performed via forcefield based scoring functions that apply CHARMM forcefield to calculates the energy of the pose-protein complex so enable the program to rank the poses

based on the scores. The program provides the results in PDBQT files that contain the poses alone without the protein active site so both protein and pose files can be opened in discovery studio and analyzed to get the best score and the best pose.

### 6.7. HDAC-6 assay

The compounds were resuspended in 100% DMSO. A series of dilutions of the compounds were prepared with 10% DMSO in HDAC assay buffer and 5  $\mu$ L of the dilution was added to a 50 $\mu$ L reaction so that the final concentration of DMSO is 1% in all the reactions. The enzymatic reactions for the HDAC enzymes were conducted in duplicate at 37 °C for 30 min in a 50  $\mu$ L mixture containing HDAC assay buffer, 5  $\mu$ g BSA, an HDAC substrate, HDAC enzyme, and a test compound. After enzymatic reactions, 50  $\mu$ L of 2 x HDAC Developer was added to each well and the plate was incubated at room temperature for an additional 15 min. Fluorescence intensity was measured at an excitation of 360 nm and an emission of 460 nm using a Tecan Infinite M1000 microplate reader.

### 6.8. Anti-proliferative activity against NCI 60 cell line panel

The human tumor cell lines of the cancer-screening panel were grown in RPMI 1640 medium containing 5% fetal bovine serum and 2 mM L-glutamine. For a typical screening experiment, cells are inoculated into 96 well microtiter plates in 100  $\mu$ L at plating densities ranging from 5,000 to 40,000 cells/well depending on the doubling time of individual cell lines. After cell inoculation, the microtiter plates are incubated at 37 °C, 5 % CO<sub>2</sub>, 95% air and 100% relative humidity for 24 h prior to addition of experimental drugs. After 24 h, two plates of each cell line are fixed *in situ* with

trichloroacetic acid (TCA), to represent a measurement of the cell population for each cell line at the time of compound addition (Tz). Experimental drugs are solubilized in dimethyl sulfoxide at 400-fold the desired final maximum test concentration and stored frozen prior to use. At the time of drug addition, an aliquot of frozen concentrate is thawed and diluted to twice the desired final maximum test concentration with complete medium containing 50 µg/mL gentamicin. Additional four, 10-fold or ½ log serial dilutions are made to provide a total of five drug concentrations plus control. Aliquots of 100 µL of these different drug dilutions are added to the appropriate microtiter wells already containing 100 µL of medium, resulting in the required final drug concentrations.

Following drug addition, the plates are incubated for an additional 48 h at 37 °C, 5% CO<sub>2</sub>, 95% air, and 100% relative humidity. For adherent cells, the assay is terminated by the addition of cold TCA. Cells are fixed in situ by the gentle addition of 50 mL of cold 50% (w/v) TCA (final concentration, 10% TCA) and incubated for 60 min at 4 °C. The supernatant is discarded, and the plates are washed five times with tap water and air dried. Sulforhodamine B (SRB) solution (100 µL) at 0.4% (w/v) in 1% acetic acid is added to each well, and plates are incubated for 10 min at room temperature. After staining, the unbound dye is removed by washing five times with 1% acetic acid and the plates are air dried. The bound stain is subsequently solubilized with 10 mM trizma base, and the absorbance is read on an automated plate reader at a wavelength of 515 nm. For suspension cells, the methodology is the same except that the assay is terminated by fixing settled cells at the bottom of the wells by gently adding 50 µL of 80% TCA (final concentration, 16% TCA).

#### Declaration of interest

The authors have declared no conflict of interests.

#### Acknowledgment

I would like to express my appreciation to the National Cancer Institute, USA for performing the *in vitro* 60-cell lines anticancer assay and would like to thank Center for Drug Discovery Research and Development, Ain Shams University, for performing the NMR spectroscopy.

#### Funding

This research did not receive any specific grant from funding agencies in the public, Commercial or not-for-profit sectors.

#### Author Contributions

Heba M.Hesham reviewed the literature and prepared the manuscript. D. S. Lasheen revised the manuscript. K. A. M. Abouzid supervised the preparation of the manuscript. All the authors reviewed the manuscript.

#### 6. REFERENCES

1. De Schepper, S. *et al.* Inhibition of histone deacetylases by chlamydocin induces apoptosis and proteasome-mediated degradation of survivin. *J. Pharmacol. Exp. Ther.* **304**, 881–888 (2003).
2. Khan, O. & Thangue, N. B. La. REVIEW HDAC inhibitors in cancer biology : emerging mechanisms and clinical applications. *Immunol. Cell Biol.* **90**, 85–94 (2012).
3. Bolden, J. E., Peart, M. J. & Johnstone, R. W. Anticancer activities of histone deacetylase inhibitors. *Nat. Rev. Drug Discov.* **5**, 769–784 (2006).
4. Kawai, H., Li, H., Avraham, S., Jiang, S. & Avraham, H. K. Overexpression of histone deacetylase HDAC1 modulates breast cancer progression by negative regulation of estrogen receptor  $\alpha$ . *Int. J. Cancer* **107**, 353–358 (2003).
5. Condorelli, F., Gnemmi, I., Vallario, A., Genazzani, A. A. & Canonico, P. L. Inhibitors of histone deacetylase (HDAC) restore the p53 pathway in neuroblastoma cells. *Br. J. Pharmacol.* **153**, 657–668 (2008).
6. Nassar, D. & Blanpain, C. Cancer Stem Cells: Basic Concepts and Therapeutic Implications. *Annu. Rev. Pathol. Mech. Dis.* **11**, 47–76 (2016).
7. Kumar, B., Yadav, A., Lang, J. C. & Teknos, T. N. Suberoylanilide hydroxamic acid ( SAHA )

- reverses chemoresistance in head and neck cancer cells by targeting cancer stem cells via the downregulation of Nanog. *Genes and Cancer* **6**, 169–181 (2015).
8. Shen, D., Pouliot, L. M., Hall, M. D. & Gottesman, M. M. Cisplatin Resistance: A Cellular Self-Defense Mechanism Resulting from Multiple Epigenetic and Genetic Changes. *pharmacol rev* **64**, 706–721 (2012).
9. Bertrand, P. Inside HDAC with HDAC inhibitors. *Eur. J. Med. Chem.* **45**, 2095–2116 (2010).
10. Li, Y., Shin, D. & Kwon, S. H. Histone deacetylase 6 plays a role as a distinct regulator of diverse cellular processes. *FEBS J.* (2013). doi:10.1111/febs.12079
11. Itoh, Y., Suzuki, T. & Miyata, N. Isoform-Selective Histone Deacetylase Inhibitors. *Curr. Pharm. Des.* **14**, 529–544 (2008).
12. Yoon, S. & Eom, G. H. HDAC and HDAC Inhibitor: From Cancer to Cardiovascular Diseases. *Chonnam Med. J.* **52**, 1–11 (2016).
13. Roche, J. & Bertrand, P. Inside HDACs with more selective HDAC inhibitors. *Eur. J. Med. Chem.* (2016). doi:10.1016/j.ejmech.2016.05.047
14. Harris, F. & Pierpoint, L. The Search for Potent, Small-Molecule HDACIs in Cancer Treatment: A Decade After Vorinostat. *Med. Res. Rev.* **29**, 1292–1327 (2012).
15. Suzuki, T. & Miyata, N. Rational Design of Non-Hydroxamate Histone Deacetylase Inhibitors. *Mini-Reviews Med. Chem.* **6**, 515–526 (2006).
16. Suzuki, T. & Miyata, N. Non-hydroxamate Histone Deacetylase Inhibitors. *Curr. Med. Chem.* **12**, 2867–2880 (2005).
17. Rahman, F. U. *et al.* Morpholine or methylpiperazine and salicylaldimine based heteroleptic square planar platinum (II) complexes: In vitro anticancer study and growth retardation effect on E. coli. *Eur. J. Med. Chem.* **131**, 263–274 (2017).
18. Dwyer, F. P. & Mellor, D. P. *Chelating Agents, and Metal Chelates.* (1964).
19. Somasundaran, P. & Nagaraj, D. R. Chemistry and applications of chelating agents in flotation and flocculation. *Reagents Miner. Ind.* 209–219 (1984).
20. Palani, A. *et al.* Biaryl Ureas as Potent and Orally Efficacious Melanin-Concentrating Hormone Receptor 1 Antagonists for the Treatment of Obesity. *J. Med. Chem.* **48**, 4746–4749 (2005).
21. Abiraj, K., Srinivasa, G. R. & Gowda, D. C. Transfer Hydrogenation of Aromatic Nitro Compounds Using Polymer-Supported Formate and Pd-C. *Synth. Commun.* **35**, 223–230 (2005).
22. Wang, L., Feng, Y., Xue, J. & Li, Y. Synthesis and characterization of novel porphyrin Schiff bases. *J. Serbian Chem. Soc.* **73**, 1–6 (2008).
23. Jaiswal, S., Mishra, A. P. & Srivastava, A. The Different Kinds of Reaction involved in the synthesis of 2-substituted Benzothiazole and its derivatives: A Review. *Res. J. Pharm. Biol. Chem. Sci.* **3**, 631–641 (2012).
24. Pingree, R. *et al.* Synthesis, molecular docking, and QSAR study of sulfonamide-based indoles as aromatase inhibitors. *Eur. J. Med. Chem.* **143**, 1604–1615 (2018).
25. Hepperle, M. *et al.* Mono N-arylation of piperazine(III): Metal-catalyzed N-arylation and its application to the novel preparations of the antifungal posaconazole and its advanced intermediate. *Tetrahedron Lett.* **43**, 3359–3363 (2002).